JOURNAL OF MASS SPECTROMETRY, VOL. 32, 864–874 (1997)

Ion–Molecule Reactions of Halocarbon Cations with Polycyclic Aromatic Hydrocarbons in a Quadrupole Ion Trap Part I—Differentiation of Structural Isomers

Andrew A. Mosi, William R. Cullen and Guenter K. Eigendorf*
Department of Chemistry, University of British Columbia, Vancouver, BC, V6T 1Z1, Canada

Ion–molecule reactions between polycyclic aromatic hydrocarbons (PAHs) and ions (R^+) generated from halogenated hydrocarbons (dichloromethane, chloroform, carbon tetrachloride, 1,1-dichloroethane, difluoromethane and 1,1-difluoroethane) in a quadrupole ion trap were used to differentiate a series of structural isomers of PAHs. This differentiation was based on the formation of $[M + R]^+$ and $[M + R - HX]^+$ products (X = Cl, F) between the halocarbon ions (R^+) and PAH molecules (M). Halomethanes were found to give rise predominantly to the elimination products $[M + R - HX]^+$, while the haloethanes also yielded significant amounts of the $[M + R]^+$ adducts. Differences in the ionization energies of the PAH isomers seem to be partially responsible for this differentiation process. Collision-induced dissociation experiments also revealed structural differences in the adducts of different PAH isomers. © 1997 by John Wiley & Sons, Ltd.

J. Mass Spectrom. **32**, 864–874 (1997)
No. of Figures: 9 No. of Tables: 9 No. of Refs: 26

KEYWORDS: polycyclic aromatic hydrocarbons; isomer differentiation; ion–molecule reactions; halocarbon ions; quadrupole ion trap

INTRODUCTION

Polycyclic aromatic hydrocarbons (PAHs) comprise a large class of compounds that can be found ubiquitously in the environment originating from incomplete combustion processes,[1] from petrogenic sources[1] and occasionally from large industrial point sources such as aluminum smelters operating with Soderberg electrodes.[2] Environmental concerns are predominantly associated with the mutagenic or carcinogenic properties associated with many of these compounds.[3] Their toxicological properties are often isomer specific. For instance, some PAHs, such as benzo[*a*]pyrene, are strong carcinogens whereas others, such as benzo[*e*]pyrene, are non-carcinogenic.[3] Consequently, an important aspect of PAH environmental analyses should be the ability to differentiate between structural isomers and their analogues. The combination of gas chromatography with mass spectrometry (GC/MS) employing electron ionization (EI) is a widely used technique for the analysis of complex PAH mixtures. However, since EI mass spectra of most PAH isomers are virtually identical, isomer differentiation is only possible via GC retention time matches with authentic standards. Consequently, PAHs for which standards are not available, or that co-elute with other compounds, cannot be identified using this standard technique. In order to obtain isomer differentiation it is necessary to generate mass spectra characteristic of the individual isomers.

Isomer differentiation of some PAHs by MS has been reported using positive chemical ionization with dimethyl ether[4,5] and negative chemical ionization with carbon dioxide[6,7] and oxygen.[8,9] Unfortunately, the last two techniques are strongly affected by the presence of traces of air and moisture in the mass spectrometer[10] and by surface-catalyzed reactions.[11] Tandem mass spectrometry has also been employed for differentiation of isomeric PAHs based on intensity variations of fragment ions,[12] molecular ions, protonated molecules[13] and doubly charged fragment ions.[14] Since these techniques rely upon measurements of ion ratios rather than the production of characteristic ions, they have only been used to differentiate between isomeric PAH standards, and have not been applied to the analysis of the complex PAH mixtures found in environmental samples. The purpose of this investigation was to find a sensitive GC/MS technique that would be able to generate characteristic isomer-specific mass spectra for PAHs.

Benzene has been shown to undergo electrophilic aromatic substitutions in the gas phase similarly to those occurring in solution.[15] Formation of gas-phase

* *Correspondence to*: G. K. Eigendorf, Department of Chemistry, University of British Columbia, Vancouver, BC, V6T 1Z1, Canada.
Contract grant sponsor: Royal Canadian Military College Environmental Sciences Group.
Contract grant sponsor: Department of Indian and Northern Development (DIAND).
Contract grant sponsor: National Science and Engineering Research Council of Canada.

CCC 1076–5174/97/080864–11 $17.50

Received 14 February 1997
Accepted 13 May 1997

adducts between dichloromethane and naphthalene has been demonstrated using a high-pressure ion source[16] and various other halogenated hydrocarbons have been used as reagent gases for chemical ionization.[17–21] However, to the best of our knowledge, ion–molecule reactions of isomeric PAHs with halogenated hydrocarbons have not been reported so far.

A mass spectrometer that is becoming more commonly used for environmental trace analysis is the quadrupole ion trap. Compared with sector or linear quadrupole instruments it generally affords higher sensitivity because the ions are generated and detected in the same location, reducing transmission losses.[22] Initially we attempted to perform the earlier reported[4,5] isomer differentiation experiments on a GC/MS ion trap using dimethyl ether as a reagent gas, but failed to achieve the reported formation of the characteristic $[M + CH_2OCH_3]^+$ adduct observed in a standard ion source. Lack of adduct formation in ion traps, when compared with standard sources, has been attributed to differences in gas pressures in the ion-forming regions.[23] Chemical ionization (CI) in an ion trap is performed at a reagent gas pressure of $\sim 10^{-5}$ mbar whereas in a conventional ion source it occurs at 0.1–1.0 mbar. The higher pressure regime of a standard CI source is more inductive to stabilization of adducts.[18] However, an ion trap has the advantage of allowing ion–molecule reactions with a mass-selected reagent ion, or a range of ions, that are formed during the ionization of the reagent gas. This selectivity offers an advantage particularly when the desired adduct-forming reagent ion is not the predominant one. The selectivity of the ion trap coupled with its high sensitivity led us to search for reagents that might form specific adducts with PAHs in the low-pressure environment of the trap, and at the same time allow isomer differentiation.

This paper reports the development of a series of sensitive GC/CI ion-trap MS techniques using halocarbon reagent gases that permit the detection and isomer differentiation of PAHs.

EXPERIMENTAL

Standards and reagents

A standard mixture of 16 PAHs (2000 μg ml^{-1} each) (naphthalene, acenaphthene, acenaphthylene, fluorene, phenanthrene, anthracene, fluoranthene, pyrene, benz[*a*]anthracene, chrysene, benzo[*b*]fluoranthene, benzo[*k*]fluoranthene, benzo[*a*]pyrene, indeno[1,2,3-*cd*]pyrene, dibenz[*a,h*]anthracene and benzo[*ghi*]perylene) was obtained from Supelco (Oakville, ON, Canada) and diluted with toluene to give 1–50 μg ml^{-1} solutions. The perdeuterated PAHs anthracene-d_{10} and acenaphthene-d_{10} were obtained from CIL (Woburn, MA, USA). Individual standards for 9,10-dihydroanthracene, 9,10-dihydrophenanthrene, tetracene, triphenylene, benzo[*e*]pyrene and perylene were obtained from Aldrich (Milwaukee, WI, USA).

Dichloromethane, chloroform (HPLC grade, Fisher Scientific, Nepean, ON, Canada), chloroform-d_3 (CIL), carbon tetrachloride (BDH, Toronto, ON, Canada) and 1,1-dichloroethane (Fisher Scientific, Fair Lawn, NJ, USA) were used to generate the corresponding reagent gases by volatilization into the ion trap via a Negretti (Fareham, Hants., UK) needle valve. Difluoromethane (PCR Research Chemicals, Gainsville, FL, USA) and 1,1-difluoroethane (Aldrich) were supplied to the ion trap from lecture bottles equipped with regulators.

Apparatus

All experiments were performed on a Saturn 4D GC/MS/MS system (Varian, Walnut Creek, CA, USA) equipped with a Wave-Board for the generation of user-defined waveforms for application to the ion-trap electrodes.

Gas chromatography was performed using a DB5 capillary column (30 m × 0.25 mm i.d., 0.25 μm film thickness) from J&W (Folsom, CA, USA) that was inserted directly into the ion trap through a transfer line maintained at 280–290 °C.

Procedure

Gas chromatography. Introduction of the samples was performed via splitless injection at 290 °C. The GC column temperature program was initial temperature 90 °C for 0.1 min followed by a 6 °C min^{-1} ramp to 280 °C, a hold at 280 °C for 1 min and then a 20 °C min^{-1} ramp to 300 °C and a hold for 20 min. Helium was used as the carrier gas at a linear velocity of 32 cm s^{-1}, corresponding to a flow rate of $\sim$1 ml min^{-1} into the ion trap.

Ion trap. The ion trap used could only be operated in the positive ion mode, thus all results reported here refer to positive ions only. The trap temperature was maintained between 220 and 255 °C. No significant changes in the gas-phase reactions were observed over this temperature range. The reagent vapours introduced into the trap were ionized with an electron beam of 70 eV. The multiplier voltage was optimized to give a gain of 10^5. The vacuum conditions were monitored via the intensity of the background spectrum (air, water) as this instrument is not equipped with a vacuum gauge.

The primary variable parameters for chemical ionization in the Saturn 4D ion trap are the reagent gas ionization time (IT), the reaction time (RT) between sample molecules and ionized reagent gas and the ionization (ISL) and reaction (RSL) storage levels. IT values can be varied from 1 to 2500 μs and RT from 1 to 128 ms. These parameters can be kept at fixed values or allowed to change automatically via an automatic reaction control (ARC) function. ARC varies the values of IT and RT to obtain an optimal number of target ions. Experiments were performed using both manual and ARC methods. If more than one type of reagent ion is formed during the ionization of a specific reagent gas, the values of IT and RT may affect the relative ratio of these ions. Consequently, IT and RT may have to be optimized manually to obtain a desired distribution of reagent ions. The relative ratios of reagent ions is also

influenced by the amount of reagent gas introduced into the trap.

The ionization storage level (ISL) represents the low-mass cut-off. Ions below this value will be automatically ejected from the trap.

When required, isolation of specific mass reagent ions for $m/z > 60$ was achieved by incorporating a Wave-Board generated MS/MS scan function.

The reaction storage level (RSL) is the lowest mass that is stored during the reaction period. The RSL level can also be adjusted to prevent reaction with unwanted low-mass ions. It is also possible to remove high-mass ions prior to the reaction period with the selected ejection chemical ionization (SECI) function.[24] This is achieved by applying a low-frequency square wave to the end-caps of the trap.

In this paper, the term 'chemical ionization' (CI) will refer to the reaction of an analyte with all ions produced during the ionization of a reagent gas, whereas the term 'ion–molecule reaction' assumes isolation of reagent ions of a specific mass followed by reaction with an analyte.

Collision-induced dissociation (CID) experiments on adducts and elimination products were performed by applying the MS/MS scan function after CI. A 1 u mass window was used to select the precursor ions. Fragmentation was achieved with the carrier gas using a non-resonant excitation waveform at 55–60 V for 10 ms.

RESULTS AND DISCUSSION

Formation of reagent ions

The major reagent ions (R^+) produced during ionization of the halocarbon gases are listed in Table 1. For the chlorinated reagents characteristic isotopic ratios were observed.

When ionization of a halocarbon vapour produces more than one reagent ion (e.g. $CH_2Cl_2 \rightarrow CH_2Cl^+ + CHCl_2^+$), the relative amounts of each type of ion will depend on RT, IT and the gas pressure, as mentioned earlier. For example, for 1,1-difluoroethane, when RT was increased from 1 to 128 ms the amount of the m/z 47 CH_3CHF^+ ions increased whereas the m/z 51 and 65 ions decreased [Fig. 1(a)]. Increasing the ionization time for CH_3CHF_2 from 10 to 1000 μs gave a linear increase in the ion count for m/z 47, 51 and 65 [Fig. 1(b)]. When the amount of 1,1-difluoroethane gas introduced into the trap was increased, as measured by an increase in the total ion count (TIC), the concentration of the m/z 47 ion increased whereas the m/z 51 and 65 ions decreased [Fig. 1(c)].

The predominance of m/z 47 at higher concentrations and reaction times suggests that a transfer of F^- from the neutral CH_3CHF_2 molecule is probably an important mechanism for the formation of CH_3CHF^+

Table 1. Major reagent ions produced during electron ionization of halocarbons

Reagent	Major reagent ions R^+ (m/z)[a]
CH_2Cl_2	CH_2Cl^+ (49/51) > $CHCl_2^+$ (83/85/87)
$CHCl_3$	$CHCl_2^+$ (83/85/87)
CCl_4	CCl_3^+ (117/119/121/123)
CH_3CHCl_2	CH_3CHCl^+ (63/65) > $CHCl_2^+$ (83/85/87)
CH_2F_2	CH_2F^+ (33)
CH_3CHF_2	CH_3CHF^+ (47) > $CH_3CF_2^+$ (65) > CHF_2^+ (51)

[a] > refers to relative abundance.

Chemical ionization reactions

Halomethane reagents. The PAH isomers investigated are shown in Fig. 2. The major product type observed from chemical ionization between halomethane reagent ions (R^+) and a PAH (M) can be expressed as $[M + R - HX]^+$ (X = Cl or F), as shown for the structural isomer pair anthracene (**1a**) and phenanthrene (**1b**) when reacted with dichloromethane (Fig. 3, Table 2). For both PAHs ions are observed at m/z 191 corresponding to $[M + CH_2Cl - HCl]^+$. For phenanthrene this ion species is more prominent. In addition, ions are also observed at m/z 225/227 corresponding to $[M + CHCl_2 - HCl]^+$. The phenanthrene mass spectrum also displays small amounts of m/z 239/241, possibly due to a reaction product of m/z 97/99 ions (probably $CHCl_2CH_2^+$), which were observed in small quantities during ionization of CH_2Cl_2, followed by loss of HCl. In general, no significant amounts of the direct adduct $[M + R]^+$ were observed with any of the halomethanes investigated. A summary of products from CI reactions of four groups of PAH structural isomers with four different halomethane reagent gases is given in Table 2.

Haloethane reagents. The major products formed between haloethane reagent ions (R^+) and a PAH (M) also follow the general formula $[M + R - HX]^+$ (X = Cl or F). However, a significant difference in this case is the presence of the direct addition product $[M + R]^+$. For example, 1,1-difluoroethane and anthracene (**1a**) form $[M + R]^+$ adducts with both CH_3CHF^+ and $CH_3CF_2^+$ ions (m/z 225 and 243) but lesser amounts of the $[M + CH_3CHF - HF]^+$ elimination product at m/z 205 and no $[M + CH_3CF_2 - HF]^+$ elimination product at m/z 223 (Fig. 4 and Table 3). Phenanthrene (**1b**) leads to the formation of three elimination products, $[M + CH_3CH_2F - HF]^+$, $[M + CH_3CHF_2 - HF]^+$ and $[M + CHF_2 - HF]^+$ (m/z 209), but only one direct addition product, $[M + CH_3CHF_2]^+$ (m/z 243). A summary of products formed from four groups of PAH structural isomers and two haloethane reagents, 1,1-difluoroethane and 1,1-dichloroethane, is given in Table 3.

In examining the product ions for the various PAH isomers groups (M_r = 178, 202, 228 and 252) listed in Tables 2 and 3, one can notice that within a group of isomers there is a marked difference in the relative abundance of various product ions. For instance, for the isomer pair anthracene (**1a**) and phenanthrene (**1b**), the $[M + 47]$ and the $[M + 81]$ ions are not present in the former whereas the $[M + 13]$ ions are much lower in abundance compared with phenanthrene. For the M_r 228 series, compounds **3b** and **3c** exhibit the largest amount of $[M + R - HX]^+$ formation and the

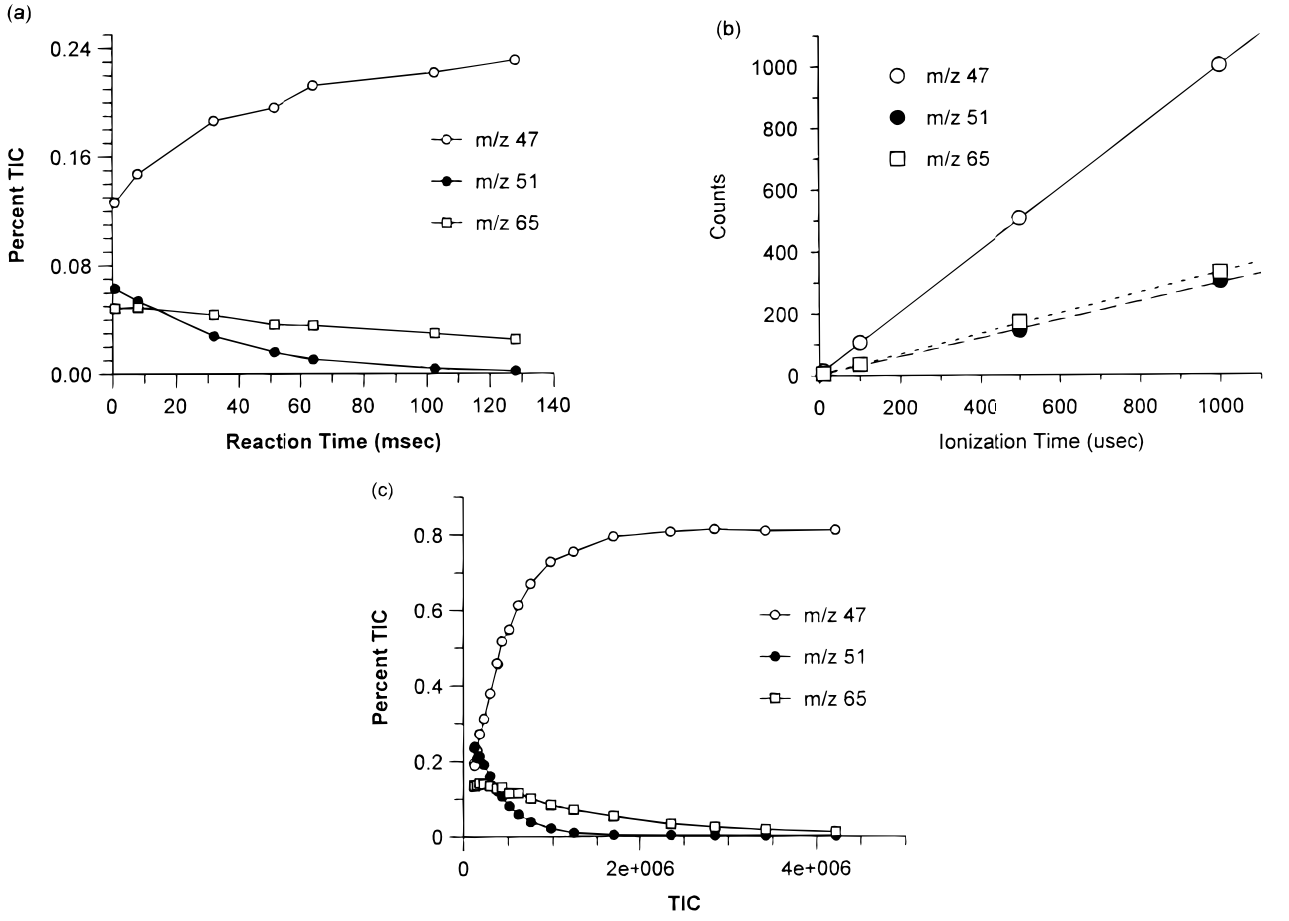

Figure 1. Effects of (a) reaction time (ms), (b) ionization time (μs) and (c) pressure (TIC) on *m/z* 47, 51 and 65 ions from 1,1-difluoroethane.

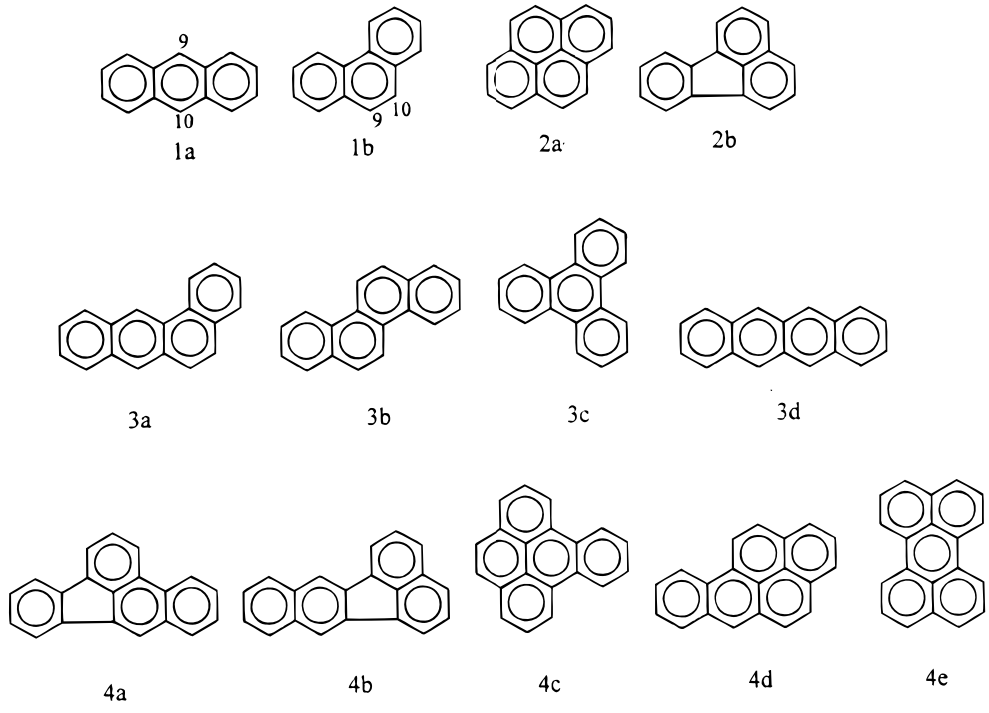

Figure 2. PAH isomers investigated.

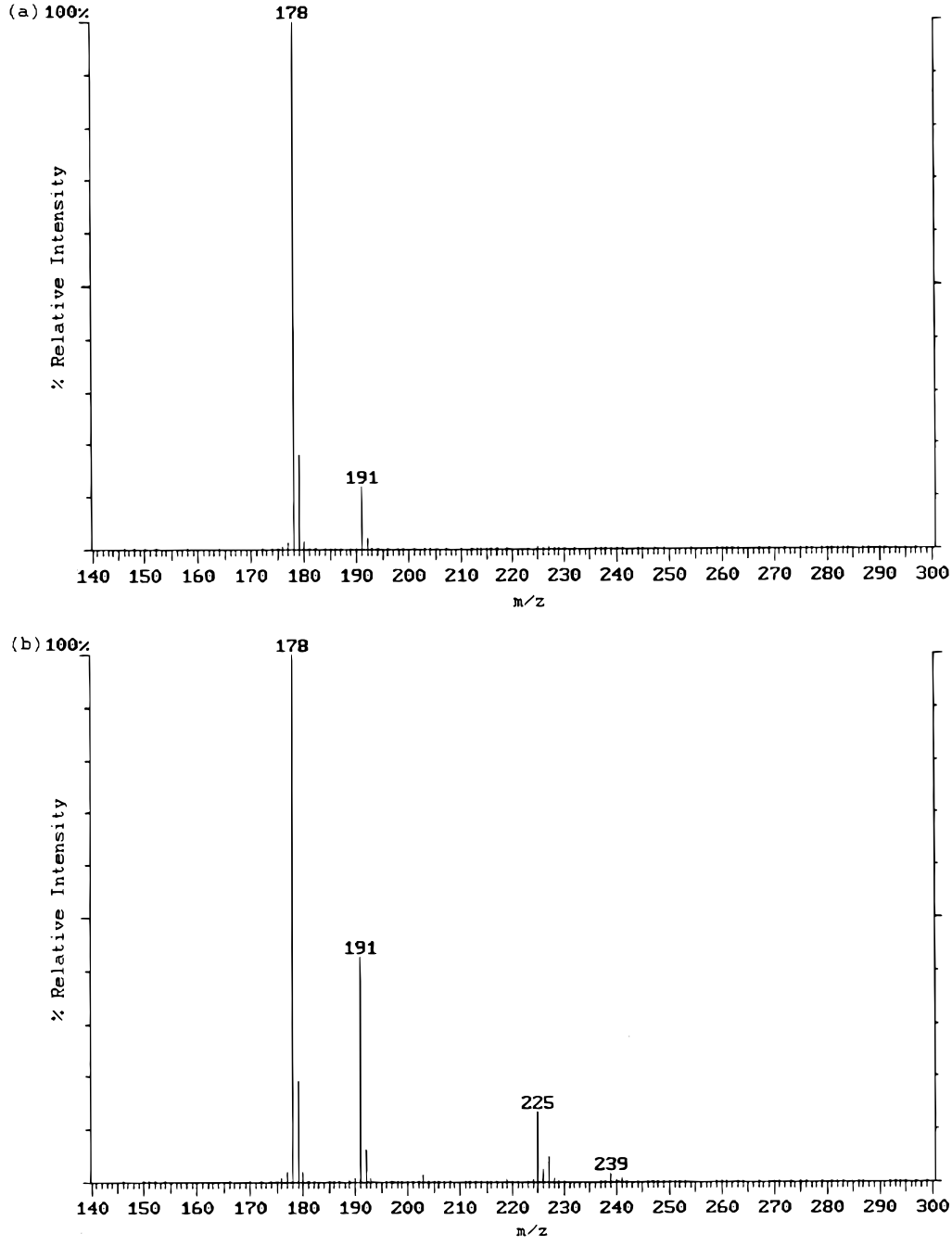

Figure 3. Dichloromethane chemical ionization mass spectra of (a) anthracene and (b) phenanthrene.

least amount of $[M + R]^+$ formation (except with $CH_3CF_2^+$). With the M_r 252 series, a decreasing trend in $[M + R - HX]^+$ formation can be noted for compounds **4a–e**.

Mechanism of adduct formation

The reaction between an aromatic system M and a positive ion R^+ is assumed to follow an electrophilic aromatic substitution mechanism (E_{AR}). In previous CI studies using benzene or naphthalene, with CH_2Cl_2 as a reagent gas,[16] the formation of $[M + 13]$ ions was attributed to $[M + CH_2Cl - HCl]^+$ and the presence of $[M + 47]$ to the elimination of H_2 from $[M + CH_2Cl]^+$. However, the $[M + 47]$ ion could also be formed through loss of HCl from $[M + CHCl_2]^+$. The use of selective ion–molecule reactions with phenanthrene (**1b**) allowed the confirmation of the latter mechanism involving elimination of HCl from $[M + CHCl_2]^+$. When $CHCl_2^+$ was preselected for the ion–molecule reaction only $[M + 13] = [M + CHCl_2 - HCl]^+$ was observed, but when CH_2Cl^+ was reacted only $[M + CH_2Cl - HCl]^+$ was formed. The lack of formation of any $[M + 47]$ ions from the reaction with CH_2Cl^+ demonstrates that H_2 is not eliminated under ion-trap conditions. The formation of $[M + 47]$ ions during CH_2Cl_2 CI must result solely from the loss of HCl from $[M + CHCl_2]^+$ rather than loss of H_2 from $[M + CH_2Cl]^+$.

Further confirmation of the HCl elimination mechanism was obtained by using $CDCl_3$ to generate $CDCl_2^+$ ions. Reaction of phenanthrene (**1b**) with these

Table 2. Major products (m/z (% rel. int.)) formed between halomethanes ions (R) and selected PAH isomers (M)

		CH_2Cl_2		$CDCl_3$	CCl_4	CH_2F_2
		$R = CH_2Cl^+$ [M + 13]	$R = CHCl_2^+$ [M + 47]	$R = CDCl_2^+$ [M + 48]	$R = CCl_3^+$ [M + 81]	$R = CH_2F^+$ [M + 13]
Compound	M^+ [a]	$[M + R - HCl]^+$	$[M + R - HCl]^+$	$[M + R - HCl]^+$	$[M + R - HCl]^+$	$[M + R - HF]^+$
Anthracene (**1a**)	178	191 (13)	225 (0)	226 (1)	259 (0)	191 (4)
Phenanthrene (**1b**)	178	191 (44)	225 (14)	226 (30)	259 (14)	191 (28)
Pyrene (**2a**)	202	215 (13)	249 (1)	250 (3)	283 (0)	215 (5)
Fluoranthene (**2b**)	202	215 (47)	249 (14)	250 (31)	283 (18)	215 (28)
Benz[*a*]anthracene (**3a**)	228	241 (12)	275 (1)	276 (2)	309 (0)	241 (5)
Chrysene (**3b**)	228	241 (25)	275 (3)	276 (20)	309 (5)	241 (12)
Triphenylene (**3c**)	228	241 (24)	275 (5)	276 (12)	—	—
Tetracene (**3d**)	228	241 (8)	275 (0)	276 (0)	309 (0)	—
Benzo[*b*]fluoranthene (**4a**)	252	265 (34)	299 (8)	300 (24)	333 (10)	265 (21)
Benzo[*k*]fluoranthene (**4b**)	252	265 (18)	299 (4)	300 (9)	333 (0)	265 (9)
Benzo[*e*]pyrene (**4c**)	252	265 (12)	299 (0)	300 (2)	333 (0)	—
Benzo[*a*]pyrene (**4d**)	252	265 (5)	299 (0)	300 (0)	333 (0)	265 (1)
Perylene (**4e**)	252	265 (3)	299 (0)	300 (1)	333 (0)	—

[a] M^+ abundance = 100%.

ions results in the production of an m/z 226/228 product corresponding to $[M + CDCl_2 - HCl]^+$. The loss of HCl rather than DCl demonstrates the elimination of hydrogen from the PAH rather than from the reactant ion.

In reverse experiments, acenaphthene-d_{10} was reacted with $CHCl_2^+$, leading to the loss of 37 u, indicating a loss of D from the PAH ring, as is expected in an E_{AR} mechanism (acenaphthene-d_{10} was used since phenanthrene-d_{10} was not available and this compound readily undergoes adduct formation).

In order for the $[M + R]^+$ adducts to be observed they must be stabilized either through collisions with neutral species (collisional stabilization) or by emission of a photon (radiative association). The former is usually the dominant process at ordinary chemical ionization pressures (0.1–1 Torr (1 Torr = 133.3 Pa)), but in the lower pressure environment of an ion trap (10^{-5} Torr) the latter mechanism could also be an important stabilization process, especially for larger molecules with 50 or more internal degrees of freedom.[25] From the data in Tables 3 and 4, it can be seen that in most cases for PAHs with similar ionization energies the higher molecular mass compounds tend to form larger amounts of $[M + R]^+$ adducts. For example, benzo[*e*]pyrene (**4c**) forms approximately four times the amount of $[M + CH_3CHF]^+$ adduct as pyrene (**2a**) (both have ionization energy $IE = 7.41$ eV).

Isomer differentiation

The ability of the halogenated hydrocarbon reagents investigated here to differentiate between PAH structural isomer pairs depends on the formation of $[M + R]^+$ adducts and $[M + R - HX]^+$ elimination products. The difference in reactivity between the structural isomers investigated was initially thought to be due to selectivity of reactive sites in a particular PAH, such as the 9,10 double bond in phenanthrene. To test this hypothesis, 9,10-dihydrophenanthrene was reacted with $CDCl_3^+$. If the reactivity of the $CDCl_3^+$ ion is selective to the 9,10 double bond then no adduct should be formed here. However, 9,10-dihydrophenanthrene actually formed slightly larger amounts of $[M + CDCl_3 - HCl]^+$ than phenanthrene, indicating that the 9,10 double bond is not essential for the formation of this ion. The reaction of $CDCl_3^+$ with 9,10-dihydroanthracene resulted in large amounts of $[M + CDCl_3 - HCl]^+$, exceeding those of both phenanthrene and 9,10-dihydrophenanthrene.

Table 3. Major products (m/z (% rel. int.)) formed between haloethanes ions (R) and selected PAH isomers (M)

	CH_3CHCl_2				CH_3CHF_2					
			$R = CH_3CHCl^+$				$R = CH_3CHF^+$		$R = CH_3CF_2^+$	
Compound	[M] M^+	[M + 1] $[M + H]^+$	[M + 27] $[M + R - HCl]^+$	[M + 63] $[M + R]^+$	[M] M^+	[M + 1] $[M + H]^+$	[M + 27] $[M + R - HF]^+$	[M + 47] $[M + R]^+$	[M + 45] $[M + R - HF]^+$	[M + 65] $[M + R]^+$
Anthracene (**1a**)	178 (100)	179 (32)	205 (11)	241 (3)	178 (100)	179 (42)	205 (10)	225 (10)	223 (10)	243 (6)
Phenanthrene (**1b**)	178 (55)	179 (68)	205 (100)	241 (2)	178 (66)	179 (100)	205 (88)	225 (0)	223 (16)	243 (7)
Pyrene (**2a**)	202 (100)	203 (33)	229 (20)	265 (4)	202 (100)	203 (46)	229 (20)	249 (20)	247 (0)	267 (20)
Fluoranthene (**2b**)	202 (64)	203 (62)	229 (100)	265 (1)	202 (55)	203 (100)	229 (86)	249 (9)	247 (18)	267 (22)
Benz[*a*]anthracene (**3a**)	228 (100)	229 (45)	255 (15)	291 (7)	228 (100)	229 (52)	255 (13)	275 (30)	273 (1)	293 (12)
Chrysene (**3b**)	228 (100)	229 (56)	255 (58)	291 (2)	228 (98)	229 (100)	255 (50)	275 (11)	273 (6)	293 (16)
Triphenylene (**3c**)	228 (100)	229 (77)	255 (74)	291 (1)	228 (42)	229 (100)	255 (16)	275 (10)	273 (2)	293 (13)
Tetracene (**3d**)	228 (100)	229 (34)	255 (7)	291 (3)	228 (100)	229 (33)	255 (15)	275 (20)	273 (8)	293 (7)
Benzo[*b*]fluoranthene (**4a**)	252 (68)	253 (95)	279 (100)	315 (10)	252 (2)	253 (100)	279 (60)	299 (25)	297 (11)	317 (30)
Benzo[*k*]fluoranthene (**4b**)	252 (100)	253 (40)	279 (35)	315 (2)	252 (100)	253 (64)	279 (25)	299 (28)	297 (3)	317 (22)
Benzo[*e*]pyrene (**4c**)	252 (22)	253 (100)	279 (42)	315 (35)	252 (2)	253 (100)	279 (20)	299 (86)	297 (4)	317 (32)
Benzo[*a*]pyrene (**4d**)	252 (100)	253 (30)	279 (2)	315 (3)	252 (100)	253 (28)	279 (1)	299 (19)	297 (0)	317 (7)
Perylene (**4e**)	252 (100)	253 (27)	279 (0)	315 (1)	252 (100)	253 (26)	279 (1)	299 (6)	297 (0)	317 (1)

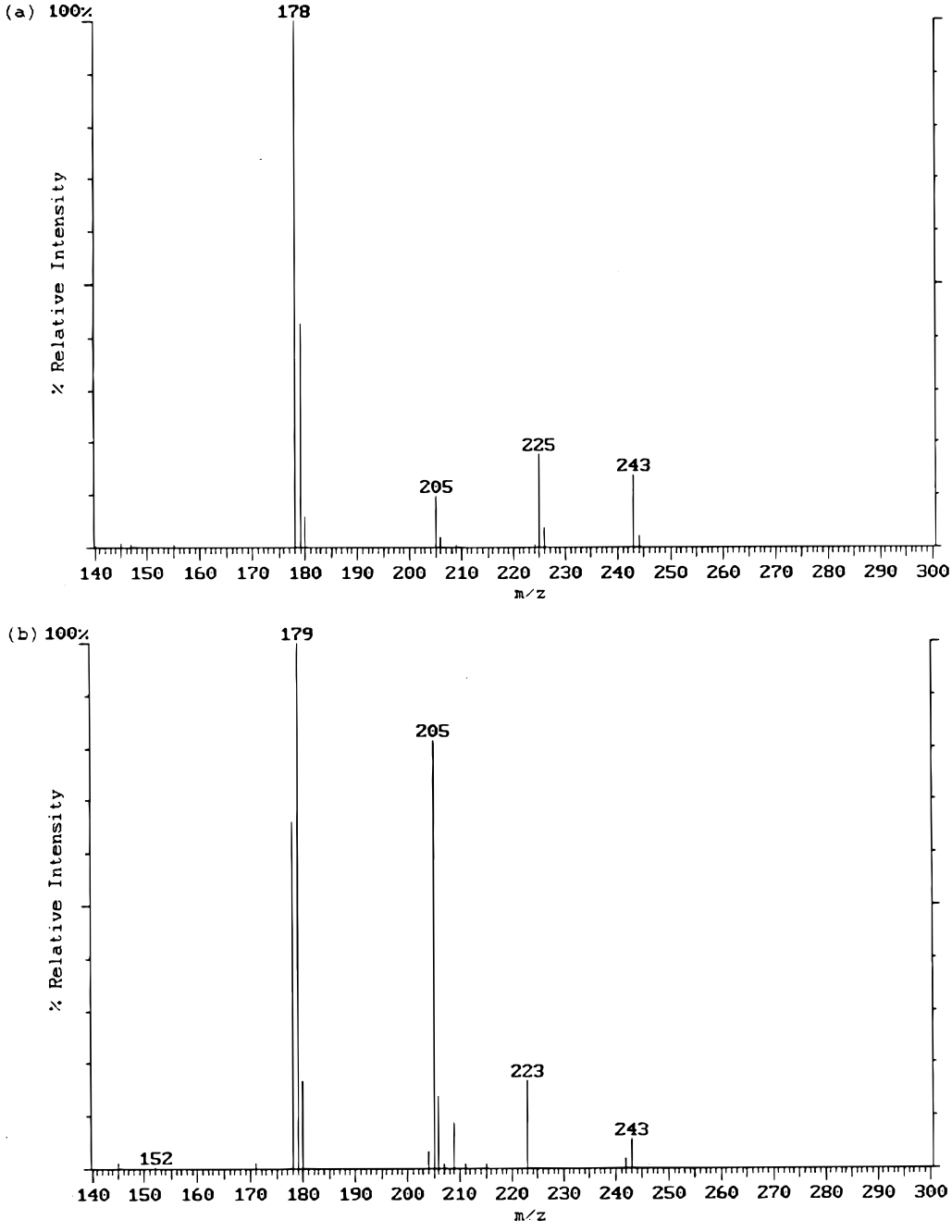

Figure 4. 1,1-Difluoroethane chemical ionization mass spectra of (a) anthracene and (b) phenanthrene.

Subsequently, differences in the physical properties, e.g. *IE*, of PAH isomers were considered to be responsible for differences in their reactivity. Using published *IE* data[26] (Table 4), it was noticed that isomers that form elimination products readily have $IE > 7.5$ eV whereas those with $IE < 7.5$ eV do not yield significant amounts of these products. This difference is clearly exemplified by the two isomer pairs anthracene (**1a**)–phenanthrene (**1b**) and pyrene (**2a**)–fluoranthene (**2b**). Phenanthrene and fluoranthene, which posses a significantly higher *IE* (7.9 eV), form $[M + R - HX]^+$ elimination products readily. Anthracene and pyrene with $IE < 7.5$ eV do not form $[M + R - HX]^+$ products readily.

When the relative amounts of $[M + R - HX]^+$ products from chloromethane ions for the 13 PAHs (**1a–4e**) were plotted as a function of their ionization energy, a positive trend with *IE* was observed (Fig. 5). From these data it can also be seen that as the number of chlorines on the reactant ion increases, the amount of elimination product decreases more rapidly with decreasing *IE*. With haloethane reagent ions a positive correlation between $[M + R - HX]^+$ formation and *IE* was also obtained (Fig. 6), although more scatter exists in the data. Linear correlations can also be obtained using energy values for the highest occupied molecular orbitals (HOMO), derived using Hückel molecular orbital theory, in place of *IE* values, since a good linear relationship can be obtained between PAH *IE* values and HOMO energy values (Table 4).

The fact that PAHs with a low *IE* do not readily form $[M + R - HX]^+$ products could suggest that

Table 4. Ionization energy (*IE*), HMO *B* values and proton affinities (*PA*) of PAHs

Compound	*IE* (eV) (exp., Ref. 25)	HOMO energy β values[a]	*PA* (kcal mol^{-1}) (exp., Ref. 25)
Anthracene (**1a**)	7.45 ± 0.03	0.41	207
Phenanthrene (**1b**)	7.86 ± 0.02	0.61	199
Pyrene (**2a**)	7.41	0.45	206
Fluoranthene (**2b**)	7.95 ± 0.04	0.62	199
Benz[*a*]anthracene (**3a**)	7.43 ± 0.03	0.45	198[c]
Chrysene (**3b**)	7.59 ± 0.02	0.52	202
Triphenylene (**3c**)	7.84 ± 0.01	0.68	198.5
Tetracene (**3d**)	6.97 ± 0.02	0.30	218
Benzo[*b*]fluoranthene (**4a**)	7.9[b]	0.60	196[c]
Benzo[*k*]fluoranthene (**4b**)	7.5[b]	0.46	198[c]
Benzo[*e*]pyrene (**4c**)	7.41	0.50	197[c]
Benzo[*a*]pyrene (**4d**)	7.12 ± 0.01	0.37	201.5[c]
Perylene (**4e**)	6.90 ± 0.01	0.35	197

[a] Calculated using Hückel molecular orbital approximations.
[b] estimated using HOMO energy values according to the linear regression equation *IE* (eV) = 2.997β + 6.115, r = 0.97.
[c] Calculated (Ref. 26).

these compounds may undergo charge exchange more readily than adduct formation. The recombination energy (*RE*) values for the reactant ions studied are shown in Table 5 (obtained from the *IE* values of neutrals[26]). These values are greater than the *IE* of PAHs investigated here, allowing for charge exchange to occur with an excess energy of ~0.1–2 eV.

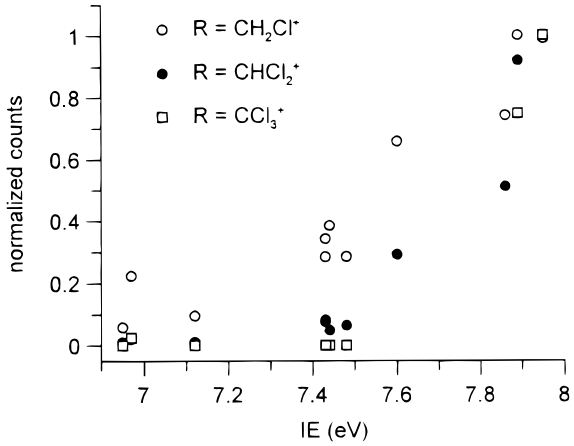

Figure 5. Effect of PAH ionization energy on the formation of $[M + R - HX]^+$ elimination products with chloromethane reagent ions.

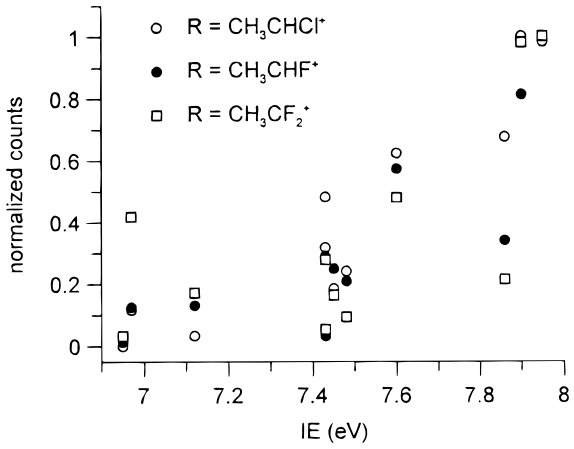

Figure 6. Effect of PAH ionization energy on the formation of $[M + R - HX]^+$ elimination products with haloethane reagent ions.

Although the formation of $[M + R]^+$ adducts with haloethane reagent ions seems to favour the lower *IE* PAHs, no direct correlation was found between adduct formation and PAH *IE* values.

Protonation of PAHs can also take place if their proton affinity (*PA*) exceeds that of the deprotonated reagent ions [R − H] (Tables 4 and 5). None of the halomethanes tested here yielded any significant amounts of PAH protonation (the [M + 1] signals were not significantly larger than the expected ^{13}C contribution), whereas the haloethanes resulted in the formation of MH^+ ions (Table 3). The formation of significant amounts of MH^+ ions with haloethanes can be explained by the lower *PA* of the [R − H] species (172–175 kcal mol^{-1} (1 kcal = 4.184 kJ)) in comparison with the *PA* of PAHs (196–207 kcal mol^{-1}). Halomethane [R − H] species have *PA* values approximating those of PAHs (193–208 kcal mol^{-1}), explaining the lack of MH^+ formation with these reagents. Interestingly, some of the PAHs with the highest *PA* values, such as **1a**, **2a** and **3d**, displayed the smallest amounts of MH^+ formation (Table 4). These three PAHs also posses low *IE* values. Consequently, PAHs with low *IE* values seem to undergo charge exchange to M^+ preferentially over

Table 5. Recombination energies (*RE*) and proton affinities (*PA*) for halocarbon ions

Ion (R^+)	*RE* (R^+) (eV)[a]	*PA* of (R—H) (kcal mol^{-1})[b]
CH_2Cl^+	8.6	208
$CHCl_2^+$	8.1	193
CCl_3^+	7.8	—
CH_2F^+	9.05	193
CH_3CHF^+	7.93	175
$CH_3CF_2^+$	7.92	174
CH_3CHCl^+	N/A[c]	172

[a] From *IP* values of neutral R from Ref. 25.
[b] Calculated using enthalpies of formation from Ref. 25.
[c] N/A not available.

either $[M + R - HX]^+$ formation or protonation, as shown in Fig. 7.

MS/MS fragmentation of adducts

For the PAH–halocarbon experiments where adducts are not observed at all or only in small amounts, the possibility exists that either adducts are initially formed but decompose before detection, or that the PAHs undergo charge exchange preferentially to adduct formation thus leading predominantly to molecular ions. To investigate possible differences in the nature of adducts formed by anthracene (**1a**) and phenanthrene (**1b**), CID experiments were performed following CI.

When the $[M + CDCl_2]^+$ *m/z* 262 adducts (minor products) of these two PAHs were fragmented via CID (60 V, non-resonant), both led to loss of HCl (*m/z* 226), but only the anthracene adduct yielded its molecular ion at *m/z* 178 (Table 6). These results seem to indicate that the anthracene $[M + R]^+$ adduct is less stable than the phenanthrene adduct and that the two adducts may be different in nature (e.g. covalent *vs.* non-covalent). The lack of an *m/z* 178 dissociation product from the CID of the phenanthrene adduct also suggests that the molecular ion normally observed during CI experiments is probably formed via charge exchange rather than via fragmentation of the adduct (unimolecular redissociation). CID on the phenanthrene $[M + CDCl_2 - HCl]^+$ *m/z* 226 adduct gave rise to *m/z* 190 from the loss of a second HCl, but once again no fragmentation to *m/z* 178 was observed. No CID experiment for *m/z* 226 could be performed with anthracene since this ion was not detectable.

Table 6. CID of $[M + R]^+$ adducts of phenanthrene and anthracene (60 V, 10 ms, non-resonant)

R^+	M	$[M+R]^+$	$[M+R-HCl]^+$	M^+
$CDCl_2^+$	Phen	100	30	0
	Anth	100	82	76

Using 1,1-difluoroethane, CID experiments were performed on the $[M + R]^+$ and $[M + R - HX]^+$ adducts of anthracene and phenanthrene for R = CH_3CF_2, CH_3CHF^+ and CHF_2^+ (Tables 7 and 8). For all three adducts anthracene displays a greater degree of fragmentation, yielding $[M + R - HF]^+$ and M^+ ions. In general, these results again indicate a lower stability for both the $[M + R]^+$ and $[M + R - HF]^+$ adducts of anthracene.

Effects of reaction time and PAH concentration on adduct formation

When a series of reaction times ranging from 10 to 128 ms were applied to PAH CI with $CDCl_3$, no significant

Table 7. CID of $[M + R]^+$ adducts of phenanthrene and anthracene (55 V, 10 ms, non-resonant)

R^+	M	$[M+R]^+$	$[M+R-HF]^+$	$[M+R-2HF]^+$	M^+
CHF_2^+	Phen	100	0	0	5
	Anth	100	0	0	45
CH_3CHF^+	Phen	n/q[a]	n/q	N/A[b]	n/q
	Anth	4	100	N/A	20
$CH_3CF_2^+$	Phen	100	40	25	32
	Anth	28	100	32	68

[a] n/q not quantifiable.
[b] N/A not applicable.

Table 8. CID of $[M + R - HF]^+$ adducts of phenanthrene and anthracene (55 V, 10 ms, non-resonant)

R^+	M	$[M+R-HF]^+$	$[M+R-2HF]^+$	M^+
CHF_2^+	Phen	100	6	4
	Anth	100	0	62
CH_3CHF^+	Phen	100	N/A[a]	2
	Anth	100	N/A	17
$CH_3CF_2^+$	Phen	100	60	1
	Anth	100	50	30

[a] N/A not applicable.

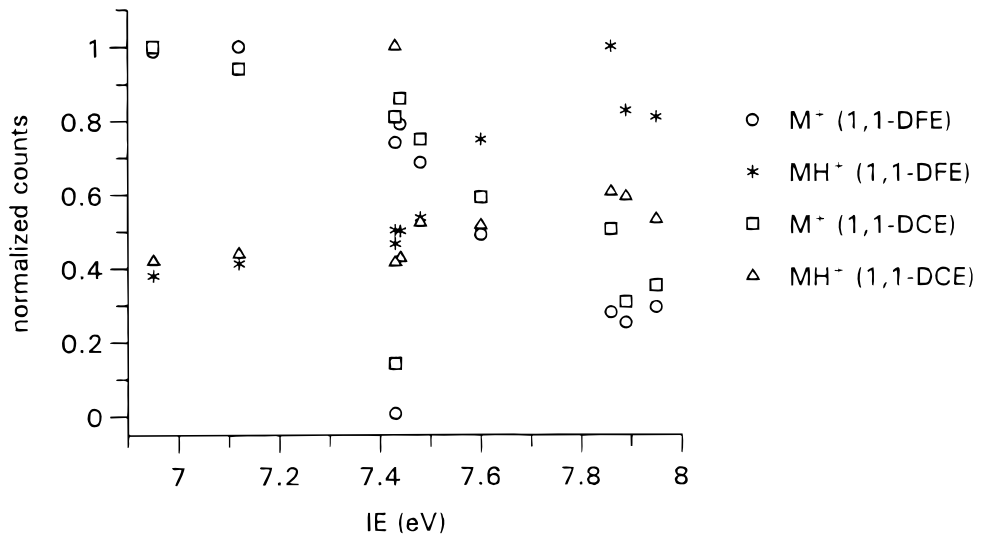

Figure 7. Effect of PAH ionization energy on the formation of M^+ and MH^+ in the presence of haloethane reagent ions (1,1-DFE = 1,1-difluoroethane; 1,1-DCE = 1,1-dichloroethane).

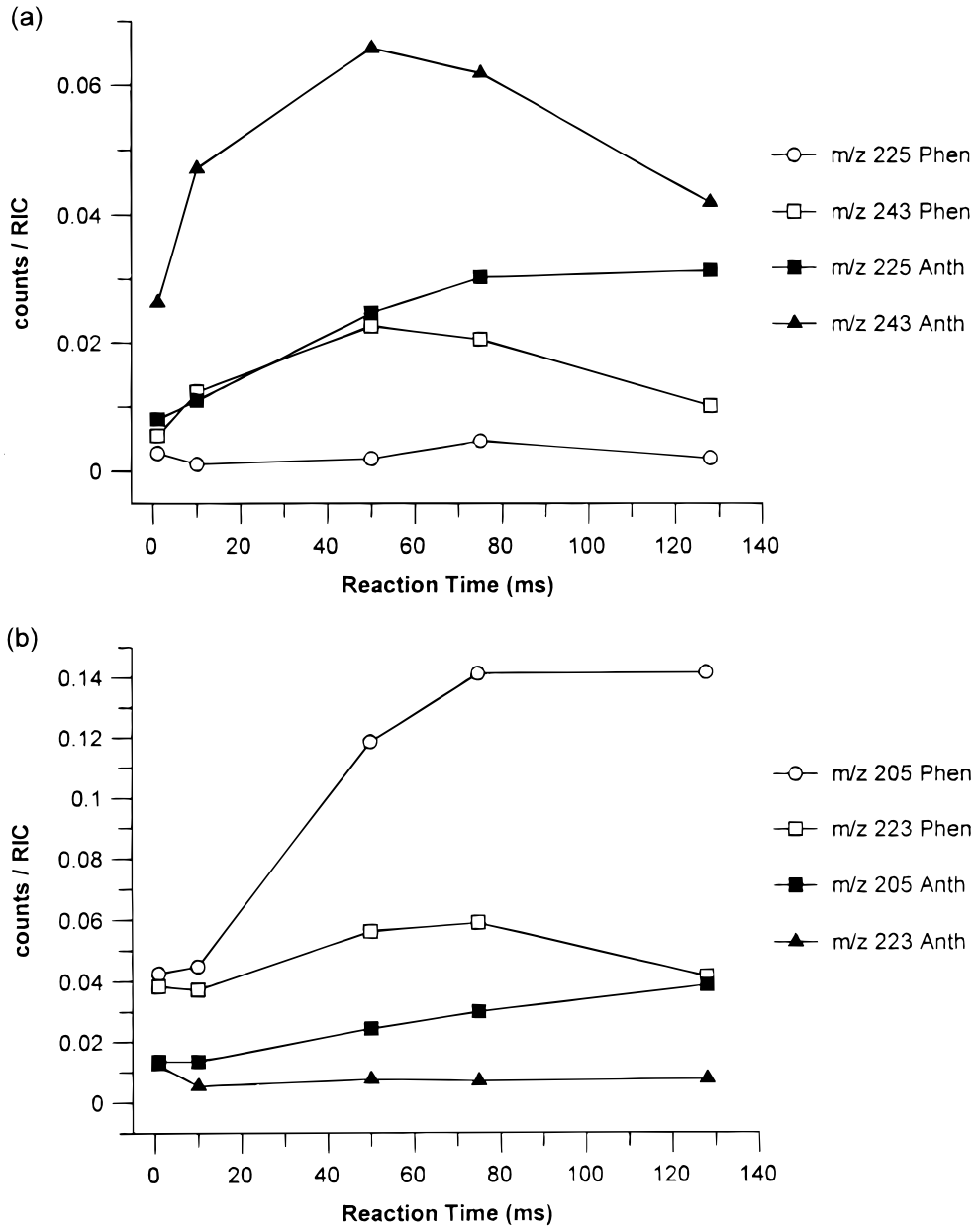

Figure 8. Effect of reaction time on the formation of (a) $[M + R]^+$ and (b) $[M + R - HF]^+$ (*m/z* 205 and 225, R = CH_3CHF^+; *m/z* 223 and 243, R = $CH_3CF_2^+$).

changes in the relative amount of adduct formation (i.e. as a percentage of TIC) were noted. However, with 1,1-DFE, increases in reaction time resulted in larger amounts of both $[M + R]^+$ and $[M + R - HF]^+$ being formed with R = CH_3CHF^+ [Figs 8(a) and (b)]. This was expected since an increase in reaction time yielded larger amounts of the CH_3CHF^+ (*m/z* 47) ion, as shown previously [Fig. 1(a)].

Table 9. Effect of sample concentration on the relative abundances (%) for major ions observed during chemical ionization with 1,1-difluoroethane

	Phenanthrene (*m/z*)						Anthracene (*m/z*)					
Amount (ng)	178	179	205	223	225	243	178	179	205	223	225	243
57 000	95	100	65	16	<1	<1	100	32	8	1	7	8
29 000	80	100	65	16	<1	3	100	35	9	2	8	8
10 000	55	100	72	13	<1	3	100	40	12	2	9	8
5000	48	100	75	12	<1	3	100	40	13	<1	10	7
572	35	100	72	8	5	2	100	40	16	1	8	4
286	35	100	75	7	5	1	100	38	13	1	8	4
100	38	100	80	5	<1	2	100	38	13	<1	8	5
50	40	100	79	8	<1	<1	100	40	16	<1	10	4

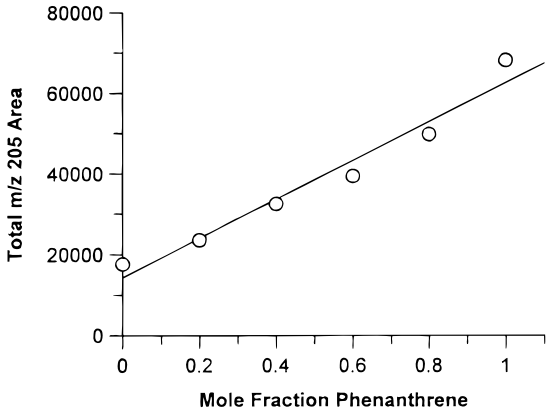

Figure 9. Effect of mole fraction composition of phenanthrene–anthracene on m/z 205 $[M + CH_3CHF - HF]^+$ during difluoroethane chemical ionization (correlation coefficient (r) = 0.98).

These results indicate that the reaction time can be an important factor in the relative amounts of adducts formed during CI when more than one reagent ion is present.

It has been found (Table 9) that under ARC conditions for a pair of isomers, e.g. phenanthrene and anthracene, a change in concentration over two or even three orders of magnitude does not significantly affect the relative abundances of the major ions discussed in this work. Thus, using mathematical correlations of the different m/z values it is possible to determine the relative amounts of each member of an isomer group. This is illustrated in Fig. 9, showing the relationship between m/z 205 $[M + CH_3CHF - HF]^+$ and mole fractions for standard mixtures of phenanthrene and anthracene.

CONCLUSIONS

The reaction of halogenated hydrocarbon ions with isomeric PAHs produced characteristic mass spectra, especially when haloethanes were employed. These results offer the potential for the identification and isomer differentiation of PAHs in complex mixtures. Furthermore, this technique can be applied towards the identification of substituted PAH isomers for which standards are not available or that co-elute. A detailed account of the application of this technique to the analysis of complex environmental samples containing PAHs will be reported in Part II.

Acknowledgements

The authors thank Varian Canada for the extended loan of the MS/MS and CI features of the Saturn 4D ion trap. They acknowledge financial support from Dr K. Reimer of the Royal Canadian Military College Environmental Sciences Group, from the Department of Indian and Northern Development (DIAND) and from the National Science and Engineering Research Council of Canada.

REFERENCES

1. *Polycyclic Aromatic Hydrocarbons in the Aquatic Environment: Formation, Sources, Fate and Effects on Aquatic Systems*. Publication No. NRCC 18981, NRCC, Ottawa (1983).
2. R. Roussel, M. Allaire and R. S. Friar, *J. Air Waste Manage. Assoc.* **42**, 1609 (1992).
3. R. G. Harvey, *Polycyclic Hydrocarbons and Carcinogens*. ACS Symposium Series 283, American Chemical Society, Washington, DC (1985).
4. T. Keough, *Anal. Chem.* **54**, 2540 (1982).
5. E. P. Burrows, *J. Mass Spectrom.* **30**, 312 (1995).
6. P. G. Sim and C. M. Elson, *Rapid Commun. Mass Spectrom.* **2**, 137 (1988).
7. C. M. Elson and P. G. Sim, *Rapid Commun. Mass Spectrom.* **4**, 37 (1990).
8. E. A. Stemmler, M. V. Buchanan, *Org. Mass Spectrom.* **24**, 94 (1989).
9. E. A. Stemmler, M. V. Buchanan, *Org. Mass Spectrom.* **24**, 205 (1989).
10. G. K. Eigendorf *et al.*, unpublished results.
11. E. A. Stemmler, *Int. J. Mass Spectrom. Ion. Processes* **142**, 178 (1985).
12. B. Shushan and R. K. Boyd, *Org. Mass Spectrom.* **15**, 445 (1980).
13. D. Chhabil, *Org. Mass Spectrom. Lett.* **28**, 470 (1993).
14. P. G. Sim, W. D. Jamieson and R. K. Boyd, *Org. Mass Spectrom. Lett.* **24**, 327 (1989).
15. D. L. Miller, J. O. Lay and M. L. Gross, *J. Chem. Soc., Chem. Commun.* 970 (1982).
16. D. C. Lane and M. McGuire, *Org. Mass Spectrom.* **18**, 494 (1983).
17. D. J. Burinsky and J. E. Campana, *Org. Mass Spectrom.* **23**, 613 (1988).
18. J. A. Stone and N. J. Moote, *Org. Mass Spectrom.* **20**, 41 (1985).
19. D. K. S. Sharma and P. Kebarle, *J. Am. Chem. Soc.* **104**, 19 (1982).
20. S. G. Lias and P. Ausloos, *Int. J. Mass Spectrom. Ion Processes* **22**, 135 (1976).
21. P. Ausloos, S. G. Lias and J. R. Eyler, *Int. J. Mass Spectrom. Ion Processes* **22**, 135 (1976).
22. J. V. Johnson, R. A. Yost, P. E. Kelley and D. C. Bradford, *Anal. Chem.* **62**, 2162 (1990).
23. J. Brodbelt, C. C. Liou and T. Donovan, *Anal. Chem.* **63**, 1205 (1991).
24. M. Wang, S. Schachterle and G. Wells, *J. Am. Soc. Mass Spectrom.* **7**, 667 (1996).
25. Y. W. Cheng and R. C. Dunbar, *J. Phys. Chem.* **99**, 10802 (1995).
26. S. G. Lias, J. E. Bartmey, J. F. Liebman, J. L. Holmes, R. D. Levin and W. G. Mallard, *J. Phys. Chem. Ref. Data*, **17**, Suppl. 1 (1988).